

FADING OF HIGH FREQUENCY RADIO SIGNALS PROPAGATING IN THE IONOSPHERE - RESULTS FROM THE JINDALEE RADAR EXPERIMENT

Kin Shing Bobby Yau

*School of Electrical and Electronic Engineering, The University of Adelaide, South Australia 5005, Australia
ksyau@eleceng.adelaide.edu.au*

ABSTRACT

The use of High-Frequency (HF) radio-wave propagation in the ionosphere is still prevalent. The ability to acquire the behaviour of the channel and the knowledge of how the channel will affect the propagating signals is imperative to ensure the reliability, and maintain adequate performance, of modern wide-bandwidth HF systems. An experiment to study the fading of HF signals propagating in the ionosphere has been conducted. Using the Jindalee Over-The-Horizon (OTH) radar, the behaviour of the ionospheric channel and wide bandwidth fading signal observations were captured. In this paper, results from the experiment will be presented, and the potential uses for the set of experimental data will be discussed.

INTRODUCTION

The use of High-Frequency (HF) radio-wave propagation in the ionosphere is still prevalent for applications such as long-range communication, target detection and commercial broadcasting. The advancement of data communication using HF, and the introduction of HF digital radio broadcasting places a greater demand on the frequency bandwidth supported by the ionospheric propagation channel [1]. The ability to acquire the behaviour of the channel and the knowledge of how the channel will affect the propagating signals is imperative to ensure the reliability, and maintain adequate performance, of modern wide-bandwidth HF systems. This is the motivation for conducting an experiment to study the fading of HF signals propagating in the ionosphere.

The experiment is focussing on one of the most undesirable characteristics of HF signals, namely the variability of the signal levels arriving at the receiver, otherwise known as fading. The main contributors to the fading of HF signals propagating in the ionosphere are: polarisation, amplitude effects and multi-path.

Polarisation fading occurs because of the rotation of the polarisation plane of the wave in a process known as Faraday rotation. Two characteristic waves, the Ordinary (O) and the Extraordinary (X), traverse through the ionosphere in slightly different path and phase speed. Since they are generally circularly polarised and opposite in direction, the resultant wave arriving at the receiver will have different polarisation compare to that of the initial wave. The dynamic nature of the ionosphere causes the ever-changing polarisation of the wave at the receiver, resulting in the effects of fading.

Another fading mechanism, amplitude fading, is caused by the movement of large-scale irregularities in the ionosphere. Depending on the position of the irregularity, the ionosphere will effectively become a concave or convex reflection layer for HF radio-wave, which causes a focussing or defocussing effects on the received signal. As the irregularity is travelling along, there will be a variation on the strength of the received signal. The effects of focussing and defocussing are shown in Fig.1.

As the name suggests, multi-path fading is caused by the presence of more than one propagation path between the transmitter and receiver. In contrast, the effects of polarisation fading and amplitude fading are apparent even where there is only a single propagation path. The waves from the different paths could either be interfering constructively or destructively when arrived at the receiver depending on the phase difference. Since the ionosphere is an ever-changing propagation medium, the phase difference between the different waves will vary in time, and therefore causes signal fading at the receiver.

Signal Fading Signatures

With the descriptions of the various mechanisms of fading in the previous section, it is worthwhile to discuss how the different types of fading can be identified. The knowledge of the signal fading signatures of the different fading mechanisms is imperative in characterising the signal fading.

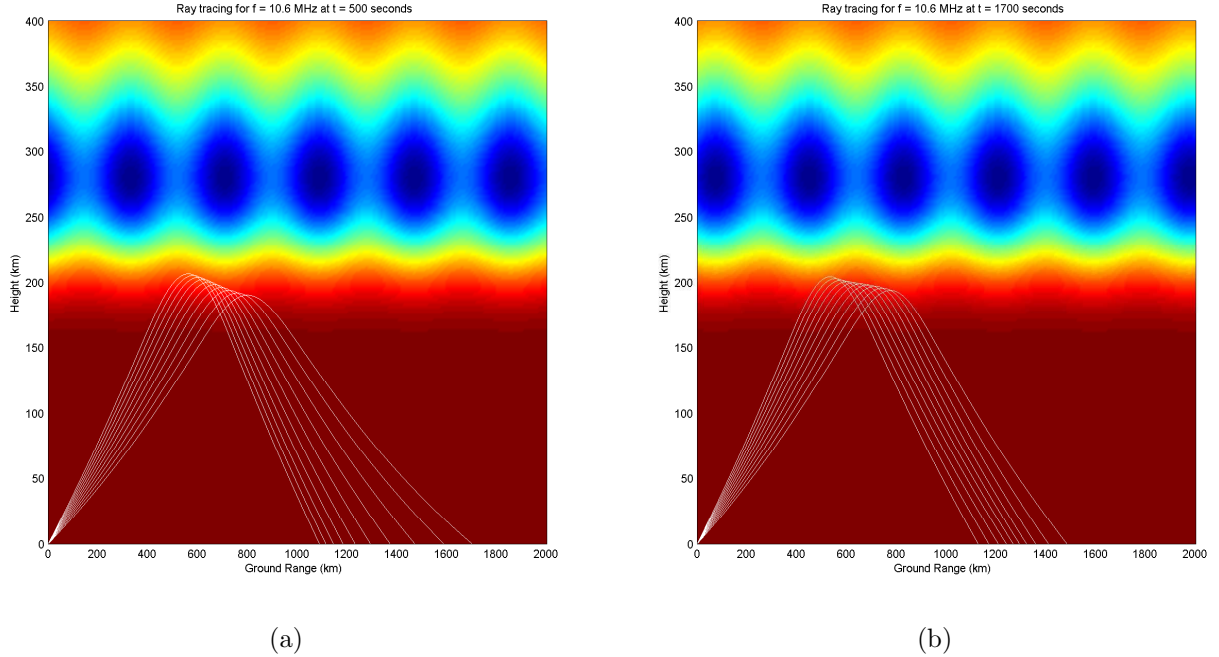


Figure 1: The effects of medium-scale travelling ionospheric disturbance (TID) on the radio-wave propagation. Ray tracing code adapted from [2] was used to generate the ray paths for a receiver located at 1220 km from the transmitter. (a) Defocussing ray paths as observed by the receiver at 1220 km. (b) Focussing ray paths as observed by the receiver at 1220 km.

For polarisation fading, it is caused by the rotation of the polarisation of the electric field. The signal strength at the receiver is dependent on the alignment between the polarisation vector and the orientation of the antenna. In the case of a dipole antenna, maximum signal strength occurs when polarisation vector of the received wave is parallel with the axis of the elements, and minimum signal when they are orthogonal. As the polarisation vector rotates, the received signal strength cycles between maximum and minimum. Now if there is a second dipole antenna that is oriented orthogonally compare to the first antenna, the time at which the maximum and minimum occurs at the second antenna will be exactly opposite to the first. i.e. Received signal strength between two orthogonal antennas will be exactly out of phase. This is the signature of polarisation fading.

Both amplitude effects fading and multi-path fading is caused by the variations of the amplitude of the wave arriving at the receiver. Therefore the same fading effects will be observed on two orthogonal antennas. i.e. Fading observed on orthogonal antennas will be in-phase.

Multi-path fading is very sensitive to the change in phase difference between the different propagation paths, as a slight change in phase difference could result in either constructive or destructive interference at the receiver. Thus it is expected that multi-path fading will produce a rapid variation in the signal amplitude. Conversely, focussing effects due to the movement of large-scale irregularities will produce the slower type of fading.

In the following sections, descriptions of the fading experiment, along with the experimental results, will be presented.

EXPERIMENTAL CAMPAIGN

The experimental campaign consists of observing the fading of HF signals propagating through the ionosphere. The main objectives of the experiment are: (1) to characterise the fading of HF radio signals propagating in the ionosphere, and (2) to understand the different mechanisms that cause the different types of fading. In this paper, preliminary results on the characterisation of the different types of fading will be presented. However, the ionosonde data recordings for the experimental period are not available at present. It is hopeful that the ionosonde data can be obtained in the near future and thus allow objective (2) to be achieved.

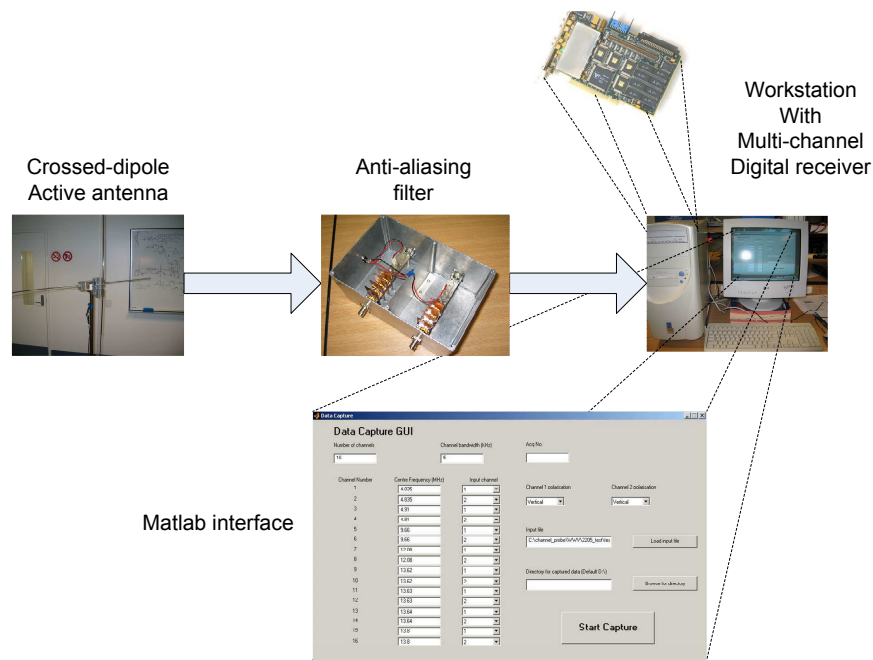


Figure 2: The compact Channel Probe

The main experimental apparatus is the compact channel probe, which was specifically developed for this experiment. Having developed the channel probe, it is imperative to obtain a suitable transmitter source to facilitate the goal of observing fading effects of HF radio signals propagating in the ionosphere. Details on the channel probe and the transmitter source will be given in the following.

Compact Channel Probe

As the main apparatus of this experiment, the compact channel probe was specifically designed to include a number of important features. The channel probe must be portable and reconfigurable, as well as having the ability to monitor dual-polarisation simultaneously. A block diagram of the channel probe is shown in Fig.2.

To achieve portability, short-dipole active antennas were used. The active circuit performs the impedance transformation of the short-antenna to that of the receiver [3], so the salient feature is the broadband performance of the active antenna over the full HF region. In addition, two dipole active antennas were arranged in the cross-dipole configuration to allow the monitoring of both vertical and horizontal polarisations.

The antennas are then connected to a dual-channel digital receiver hosted inside a computer. Software radio techniques were used to develop a fully reconfigurable channel probe, with tunable centre frequency and variable bandwidth. As the digital receiver card has two high-performance analog-to-digital converters (ADC), and several digital down-converters, the full HF band can be digitalised. To ensure that no signal aliasing was present after the ADC stage, a high performance low pass filter, with an 80dB attenuation at the Nyquist frequency of 32MHz, was used. Configuration of the channel probe can be done in software via the MATLAB Interface.

Experimental Details

Data were collected over three days between the 29th to 31st of March 2005. With the kind cooperation of Defence Science and Technology Organisation (DSTO), dedicated transmissions of HF radio signal for the sole purpose of this experiment were obtained from the Jindalee Over-the-Horizon (OTH) radar transmitter located in Alice Springs. To receive this signal, the compact channel probe was located in Darwin, and therefore the ionospheric channel consists of a 1220 km path that is almost in the north-south direction. This path was chosen because Faraday rotation is most apparent when the direction of wave propagation is aligned with the magnetic meridian.

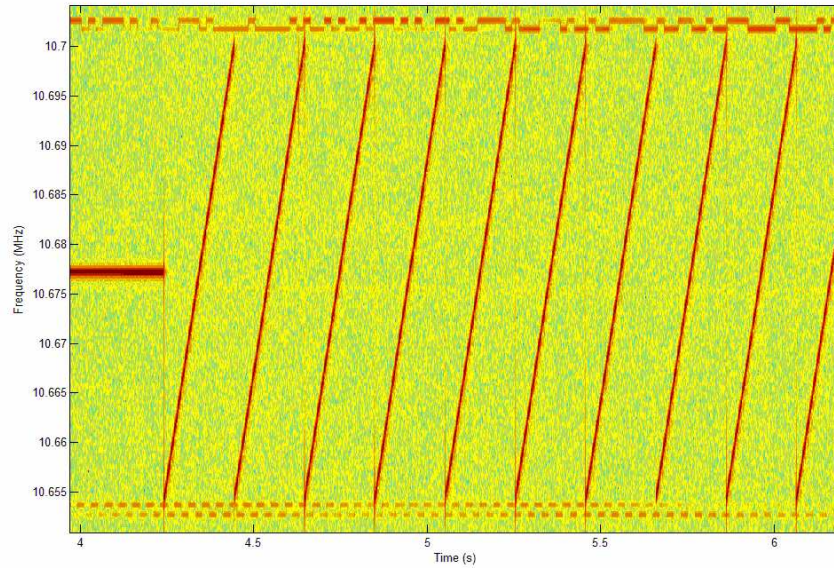


Figure 3: The chirp signal transmitted by the radar

Each day during the experiment, HF radio signals were transmitted from 15:00 until 21:00 local time, as these were the only times the radar transmitter was available for this experiment. The centre frequency and bandwidth of the signals were based on the spectral availability at the time of transmission, determined by the frequency management system (FMS) of the Jindalee OTH radar. Fortunately, on the 30th of March, two bands of frequency were available from around 16:00 until 21:00 local time. The bands were 10.677 MHz and 10.858 MHz, with bandwidths of 46 kHz and 48 kHz respectively.

Signal Characteristics

The transmitted signals were Frequency-Modulated Continuous-Wave (FMCW), otherwise known as chirp waveform. The full-bandwidth sweep rate of the signal was 5 repetitions per second, or 5 Hz. A spectrogram of the raw chirp signal is shown in Fig. 3.

Since the transmission source is an actual radar, the geographic footprint of the radar beam was changing with time. There was a 14-second cycle where the main beam of the antenna was changing between different geographic directions. Since the receiver was fixed, there were times when the signal was actually received via the side-lobe of the Jindalee radar. To overcome this problem, all the results were power-compensated with an empirically calculated factor.

RESULTS

Analysis was concentrated on the data collected on the 30th of March 2005 because it was the most complete set of data. The spectrograms of the received signal in the 10.858 MHz band at 18:51 local time is shown in Fig.4. Rapid signal fading in both polarisations is apparent. This is expected as it was during sunset at that time, when the electron density in the ionosphere was changing at a rapid rate.

Looking at the time fading and frequency fading at 18:51 in Fig.5, it is apparent that the fading was in-phase between the two polarisations. This indicates that the fading mechanism was not polarisation fading. With the short time-period and the almost periodic sinusoidal nature of time fading, this has the signature of multi-path fading due to two different propagation modes. The period of multi-path fading is quite constant at around 3 seconds, which indicates a constant rate of change in the phase path difference. This change in the phase path difference between the two modes can be attributed to the changes in the electron density profile during the time of sunset.

A closer look at the frequency fading behaviour indicates the fading was indeed caused by multi-path. The shape of the frequency fading curve corresponds to a rectified sinusoid, and therefore most likely 2 different paths exist between the transmitter and receiver. Another interesting observation is that the fading was not flat across the frequency bandwidth. This has important implications for modern high-bandwidth HF systems. That is, the fading can be reduced substantially by slight adjustment of the frequency.

Moving to around an hour later to a time well after sunset, the spectrograms of the received signal in the 10.858 MHz band at 19:43 local time are shown in Fig.6. Signal fading have become much slower in time for both polarisations, and it is clear that only a single propagation mode was present.

The time fading and frequency fading behaviour at 19:43 are shown in Fig.7. It is obvious that the fading between the two antennas is out of phase, which indicates the fading mechanism is polarisation fading. This is an important observation because polarisation fading becomes the dominant fading mechanism in a seemingly benign ionosphere. Looking at the frequency fading behaviour, the out of phase fading between the two antennas is still apparent. However the signal bandwidth is not wide enough to observe the full frequency fading bandwidth.

Fading Separation

Although the signal fading results can illustrate a clear trend on whether the primary fading mechanism is either amplitude or polarisation, it is possible to separate the two types of fading by simple data manipulation. Since we have two orthogonal receiving antennas, the received voltages can be represented by the following:

$$V_H = A(f, t) \cos(\phi(f, t)) \quad (1)$$

$$V_V = kA(f, t) \sin(\phi(f, t)) \quad (2)$$

where $A(f, t)$ is the amplitude component, $\phi(f, t)$ is the phase component, and k is the constant amplitude offset between the two antennas. The constant amplitude offset factor k was estimated by taking ratio of long time average of voltage amplitudes V_H and V_V : $k = \frac{|V_V|}{|V_H|}$.

After some simple manipulations and rearrangements, the phase and amplitude components are given by:

$$\tan \phi = \frac{V_V}{kV_H} \quad (3)$$

$$A^2 = V_H^2(1 + \tan^2 \phi) \quad (4)$$

Using (3) and (4) one can ascertain the contribution of polarisation and amplitude effects on the overall fading of the signal. The two extreme cases are: If the amplitude fading component given by (4) is varying rapidly, whereas the phase component given by (3) is steady, then amplitude fading dominates. Conversely, if the amplitude component is constant, yet the phase varies between 0 and π , then polarisation fading dominates.

The results of the fading separation for the 19:43 observations, which is the single-mode case, are shown in Fig.8. In looking at the polarisation fading component, the results between the two antennas are totally out of phase and it is very clear that the polarisation fading is the dominant mechanism at 19:43. However, a series of jumps in the amplitude component is evident. This sudden change in amplitude is attributed to the power compensation that was used to overcome the effects of the moving radar beam. The fact that this over-compensation is showing up as the amplitude fading component demonstrates that the amplitude fading separation is working as intended.

For the multi-mode case, fading separation results are shown in Fig.9. The amplitude fading component is showing the rapid fading effects that were caused by the multi-path. However, the polarisation fading component is showing mixed results. It seems to be showing a trend of polarisation fading, but at the same time showing small scale polarisation shifts. Therefore the fading separation is not working as well in the multi-path case.

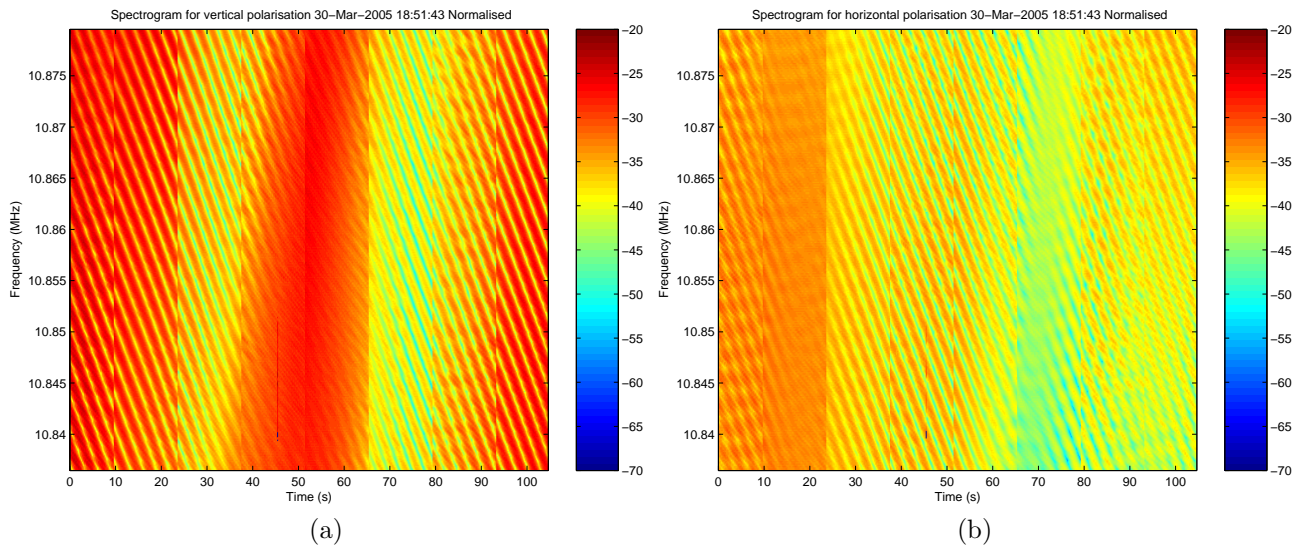


Figure 4: Spectrograms of signal commencing at 18:51 local time on the 30th March 2005. The vertical banding of 14 seconds is caused by changing of the main beam direction of the Jindalee Radar. (a) Vertical polarisation. (b) Horizontal polarisation.

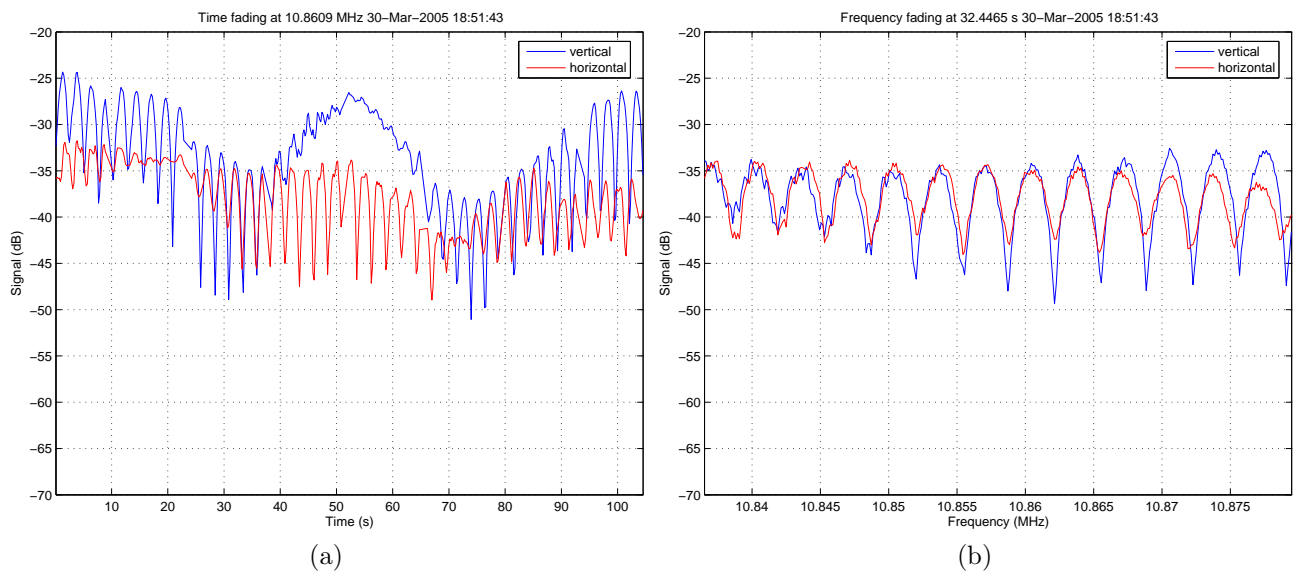


Figure 5: Time and frequency fading behaviour at 18:51 local time. (a) Time fading behaviour of the 10.8365 MHz signal commencing at 18:51 local time. (b) Frequency fading behaviour over the bandwidth at 18:52 local time.

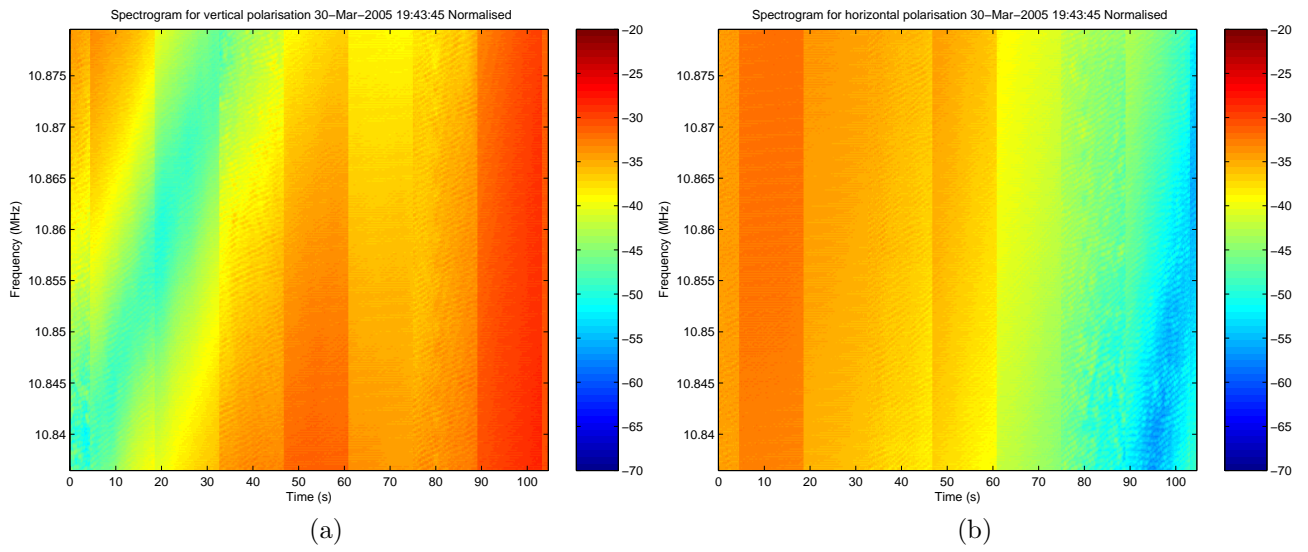


Figure 6: Spectrograms of signal commencing at 19:43 local time on the 30th March 2005. The vertical banding of 14 seconds is caused by changing of the main beam direction of the Jindalee Radar. (a) Vertical polarisation. (b) Horizontal polarisation.

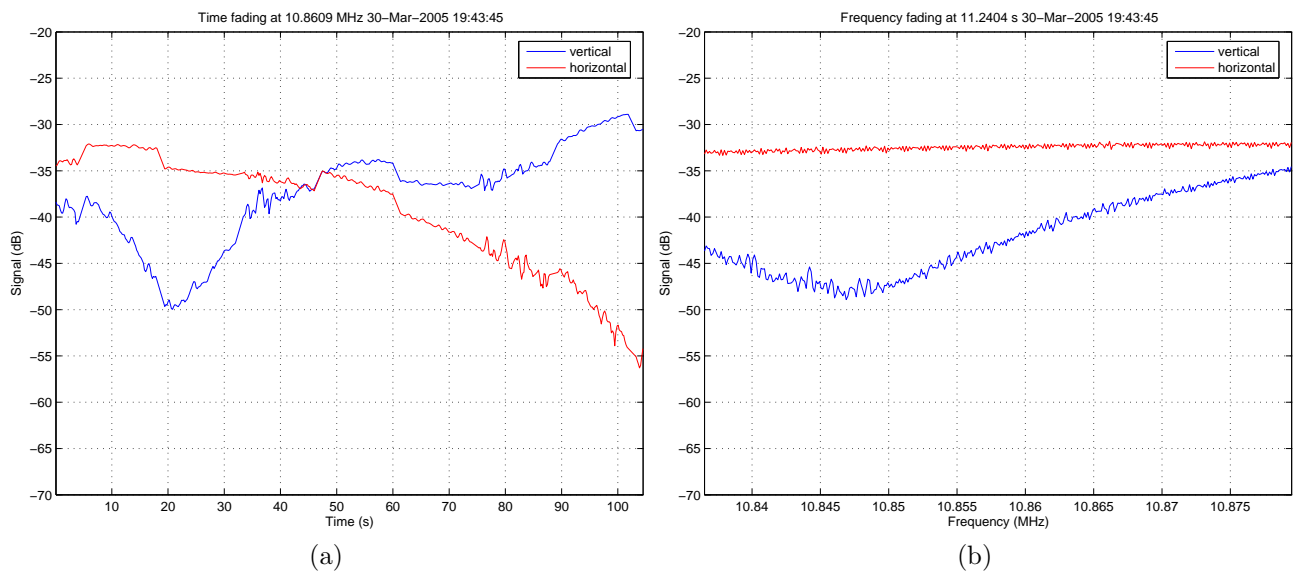


Figure 7: Time and frequency fading behaviour at 19:43 local time. (a) Time fading behaviour of the 10.8609 MHz signal commencing at 19:43 local time. (b) Frequency fading behaviour over the bandwidth at 19:43 local time.

A possible way to overcome this limitation is to exploit the fact that the transmitted signal is FMCW modulated. As all the received data have been digitalised, post-processing of the chirp signal is possible. By generating a replica of the transmitted chirp, de-sweeping of the received chirp down to baseband can be done. Using the FMCW processing techniques [4], the various receive mode time-delays are translated into different frequency bins, and thus can be separated (different modes will have greatly different time delays). After the mode separation, fading separation can then be applied to each individual modes.

DISCUSSION AND FUTURE WORK

At this stage the analysis of the acquired data have produced some interesting results. However, once the mode separation and fading separation have been properly implemented, more important results will be produced. One can then look at the effects of amplitude and polarisation fading on each of the propagation modes.

Comparisons between the signal fading data and ionosonde data will be done as soon as the ionosonde data becomes available. In doing this comparison, one will be able to discover the structure of the ionosphere during the period of rapid fading, thus identifying the types of irregularity that are causing the different types of fading. Furthermore, the ionosonde data will enable more realistic modelling of the system.

When fully analysed, the data set will become an important tool for studying the types of fading that one can expect for various ionospheric conditions. The data could also be used to test various mitigation techniques to combat signal fading. Mitigation techniques such as polarisation diversity and frequency diversity have the potential to overcome the effects of signal fading.

ACKNOWLEDGEMENTS

I thank the Defence Science and Technology Organisation (DSTO) for providing its valuable radar resources for use during this experiment. In particular, I thank Dr. Manuel Cervera for spending his valuable time in facilitating this experiment.

Gratitude also goes to my supervisor, Dr. Chris Coleman, for his unwavering support and guidance.

References

- [1] S. C. Cook. HF communication in the information age. In *Seventh International conference on HF Radio Systems and Techniques*, number 441 in Conference publication, pages 1–5. IEE, 1997.
- [2] C. J. Coleman. A ray tracing formulation and its application to some problems in over-the-horizon radar. *Radio Science*, 33(4):1187–1197, July–August 1998.
- [3] M. J. Salvati. A miniature broadband antenna. *Electronic Design*, February 1995.
- [4] D. E. Barrick. FM/CW radar signals and digital processing. Technical Report ERF 283-WPL 26, NOAA, July 1973.

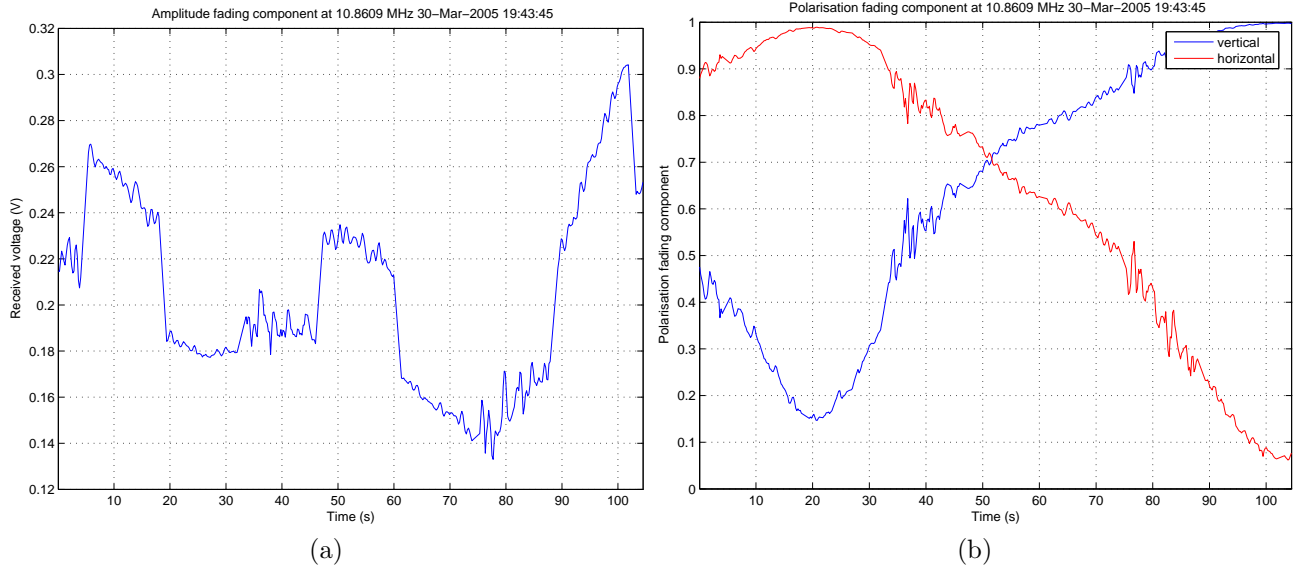


Figure 8: Fading separation for results at 19:43 local time. (a) Amplitude fading component of the 10.8609 MHz signal at 19:43 local time. (b) Polarisation fading component of the 10.8609 MHz signal at 19:43 local time.

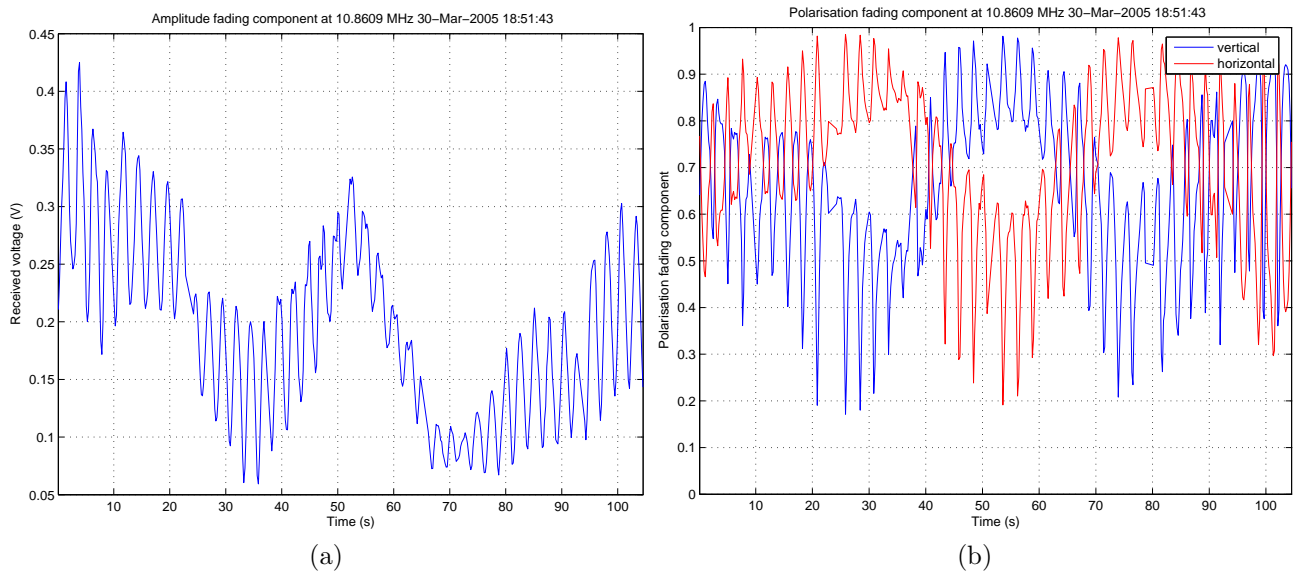


Figure 9: Fading separation for results at 18:51 local time. (a) Amplitude fading component of the 10.8365 MHz signal at 18:51 local time. (b) Polarisation fading component of the 10.8365 MHz signal at 18:51 local time.